CGMS

CGMS-35 EUM-WP-27
v1, 16 August 2007
Prepared by EUMETSAT
Agenda Item: II/7
Discussed in WG II

UPDATE ON NOWCASTING APPLICATIONS OF MSG

This paper describes a number of nowcasting applications, which are based on MSG image data and derived meteorological products. The applications range from possibilities to validate the accuracy of numerical weather prediction models with respect to the large scale circulation, e.g. the exact position of cyclones, to pre-convective identification of potentially unstable airmasses and to a detailed characterisation of the cloud formation and dissipation processes.

It is shown that the unique opportunity of the MSG spectral channels together with the quick repeat cycle of at least 15 minutes allows the derivation of advanced nowcasting products, as e.g. the instability information and the exact determination of the onset of severe convection. Especially in this area of convective storm nowcasting, a combined use of complementary observation techniques and products can be very beneficial and ensures the optimal use of the satellite data.

In conclusion, CGMS is invited to take note and to recommend the enhanced cooperation of CGMS partners in the development of further nowcasting products and techniques, especially considering the advanced utilisation of current and future geostationary satellite systems (METEOSAT, GOES, MTG, GOES-R etc.).

Update on Nowcasting Applications of MSG

1 INTRODUCTION

Since 2002 EUMETSAT operates the advanced generation of geostationary imager, the SEVIRI (Spinning Enhanced Visible and Infrared Imager) instrument onboard the Meteosat Second Generation (MSG) satellites. Two of the MSG satellites have been launched since then, and are operated under their operational names Meteosat-8 and Meteosat-9. The SEVIRI instrument was specially designed to provide enhanced nowcasting information by scanning the Earth's disk every 15 minutes in 11 spectral channels, an additional high resolution broadband visible channel is also available (Schmetz et al., 2002).

The channel selection is based on the well-known AVHRR imagers of polar orbiters, together with additional channels to allow for the detection of specific surface, cloud, and atmospheric features, e.g. identification of fog, dust storms, fires, air masses, and cloud microphysical parameters. Table 1 gives a summary of the MSG channels.

Channel	Centre (µm)	Range (µm)
VIS0.6	0.635	0.56 – 0.71
VIS0.8	0.81	0.74 – 0.88
NIR1.6	1.6	1.50 – 1.78
IR3.9	3.92	3.48 – 4.36
WV6.2	6.25	5.35 – 7.15
WV7.3	7.35	6.85 – 7.85
IR8.7	8.70	8.30 – 9.10
IR9.7	9.66	9.38 – 9.94
IR10.8	10.8	9.80 – 11.80
IR12.0	12.0	11.00 – 13.00
IR13.4	13.4	12.40 – 14.40
HRV		0.5 – 0.9

Table 1: MSG SEVIRI spectral channels

Since the launch of MSG, a number of applications have been developed to make use of these new capabilities for nowcasting, especially for the detection and prediction of severe weather.

2 MSG NOWCASTING APPLICATIONS

2.1 The Nowcasting Satellite Application Facility

Based on the 3-channel instruments of the first Meteosat generation and the exploitation of the AVHRR instrument, the Nowcasting Satellite Application Facility (SAF) hosted by the Spanish Meteorological Service (INM) in Madrid, has developed a software package for local processing of the MSG satellite information, which produce a number of products and parameters for nowcasting applications: These parameters comprise a detailed cloud analysis, air mass and layer humidity information, high resolution wind fields and a rapidly developing thunderstorm identification tool. Interested users can obtain a copy of this software from the Nowcasting SAF website at http:/nwcsaf.inm.es. For most of the products, this software needs not only the satellite data but also some fields of numerical weather prediction models, and usually needs to be tuned for a regional processing area.

An example of the cloud type product is shown in Fig. 1.

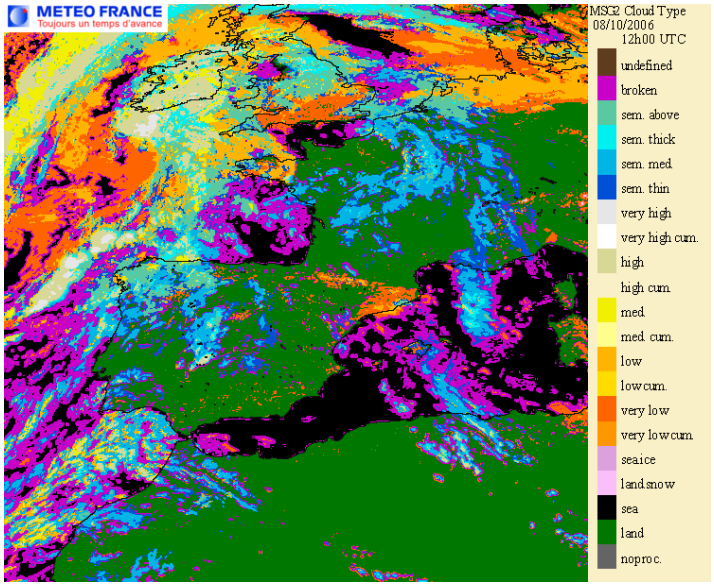

Figure 1: Example of the Nowcasting SAF Cloud Type product

2.2 Large Scale Airmass Analysis

MSG's eight thermal channels in the different atmospheric window and gaseous absorption regions (water vapour; ozone, carbon dioxide), each available every 15 minutes, already allow a close monitoring of the large-scale atmospheric processes. Furthermore, the multi-spectral combination of the MSG channels WV6.2, WV7.3, IR9.7, and IR10.8 provides the direct visualisation possibilityof different airmasses (Fig. 2) in terms of red-green-blue (RGB) colour composites. This RGB product is operationally used by several meteorological services with the aim to compare the real-time satellite data with the forecasts of numerical weather prediction models, especially to control the forecasted position and speed of cyclones.

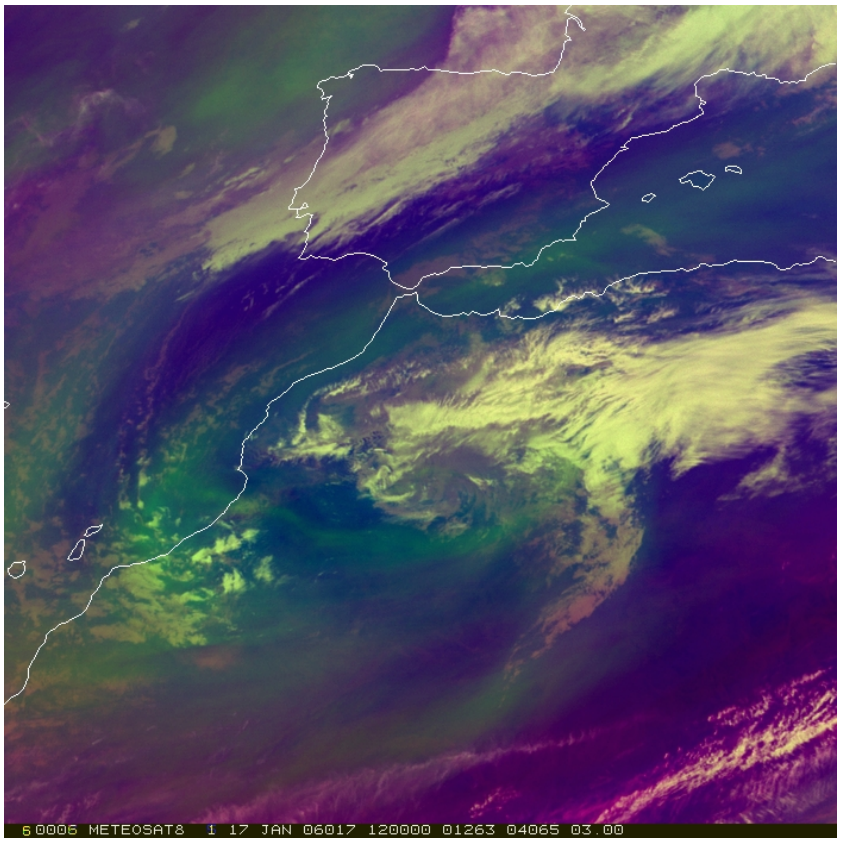

Figure 2: Airmass RGB Composite (with the temperature difference WV6.2 – WV7.3 on red, the temperature difference of IR9.7 and IR10.8 on green, and WV6.2 on blue) (17 January 2006, 1200 UTC, MSG image over North-Western Africa and the Iberian peninsula)

In this RGB combination, the ozone absorption channel IR9.7 is of special importance, as it reflects the lowering of the tropopause – and thus the local increase of stratospheric ozone – over cyclones. Ozone maxima correlate well with potential vorticitz maxima. The position of a mid-latitude cycle with centre over Morocco is well depicted by this RGB.

A more objective way to use this channel for the same purpose is the use of the Total Ozone (TOZ) product, which is derived from this channel by an optimal estimation method. The Total Ozone product is derived centrally at EUMETSAT as an average over 16 by 16 MSG pixels (~ 50 by 50 km at the subsatellite point) (Fig. 3).

The Airmass RGB is available on the EUMETSAT website www.eumetsat.int in full resolution over the entire MSG field-of-view every hour.

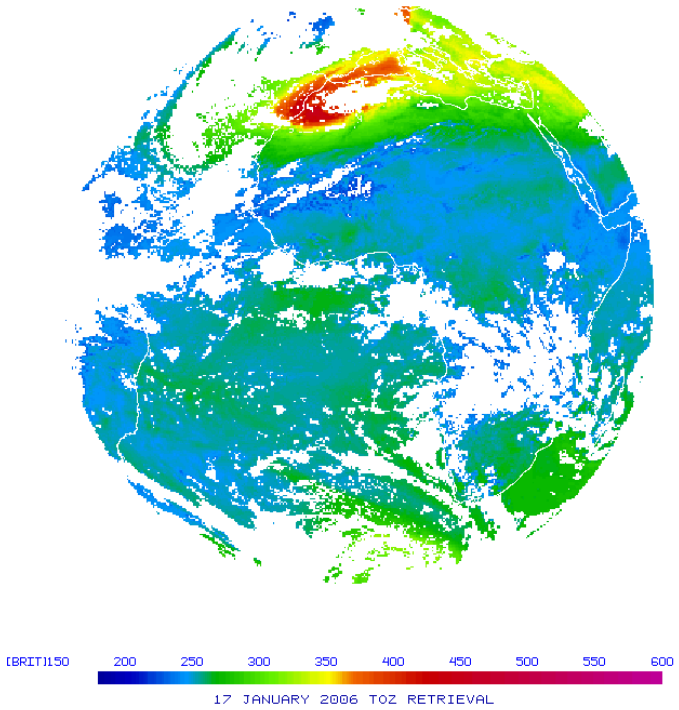

Figure 3: Full-disk view of the TOZ product for the same day and time as Fig. 2. Noteworthy is the ozone maximum over northwest Africa, which well corresponds to the above identified cyclone in this region.

2.3 Fog / Low Stratus Detection

Night-time detection of fog (or very low stratus) detection is very difficult, if not impossible, if only one infrared channel in the atmospheric window region is available, as was e.g. the case for the first generation of Meteosats. The reason for this is that fog at low atmospheric levels and the surrounding land or sea surfaces are practically at the same temperature, thus providing no temperature or brightness contrast in the IR satellite image (Fig. 4). The inclusion of the IR3.9 channel on MSG is a significant help in providing a night-time fog product: Water clouds have a lower emission at wavelengths around 3.9 um than at 11 um – for very low fog this implies that the fog appears colder in the IR3.9 channel than in IR10.8, as the total IR3.9 brightness temperature is the sum of the emission at cloud top temperature and the reflection of the much colder higher atmosphere. Fig. 5 shows examples of both channels, where the fog is much more apparent in the IR3.9 image. The usually used operational "fog product image" is the temperature difference between the IR10.8 and IR3.9 channels, where, with proper temperature scaling of the temperature difference, the fog becomes immediately apparent (Fig. 5).

The Fog RGB, which also includes this temperature difference, is available on the EUMETSAT website www.eumetsat.int in full resolution over the entire MSG field-of-view.

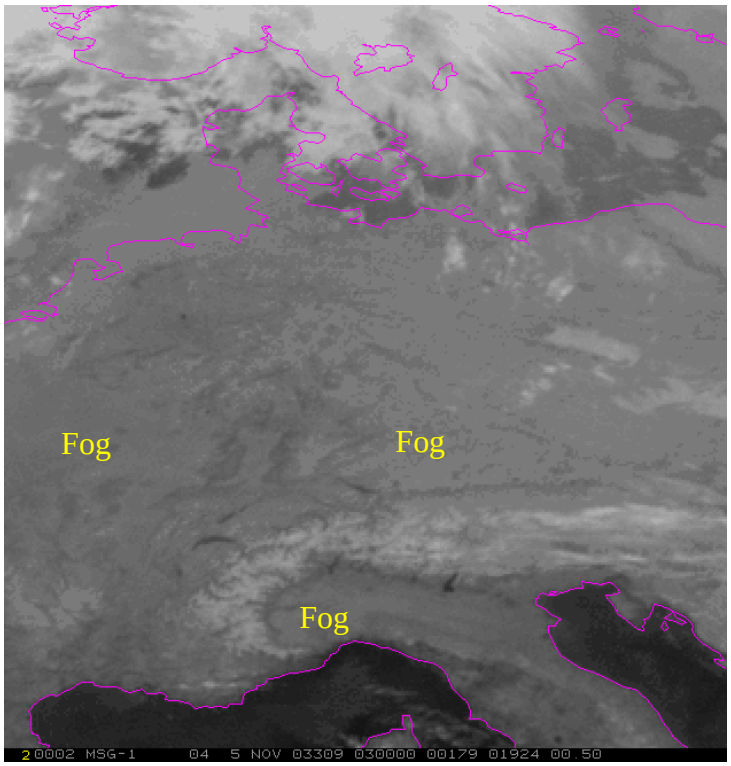

Figure 4: Night-time view of channel IR10.8 over Central Europe – the detection of fog or low stratus patches in the marked areas is difficult if not impossible. (05 November 2003, 0300 UTC)

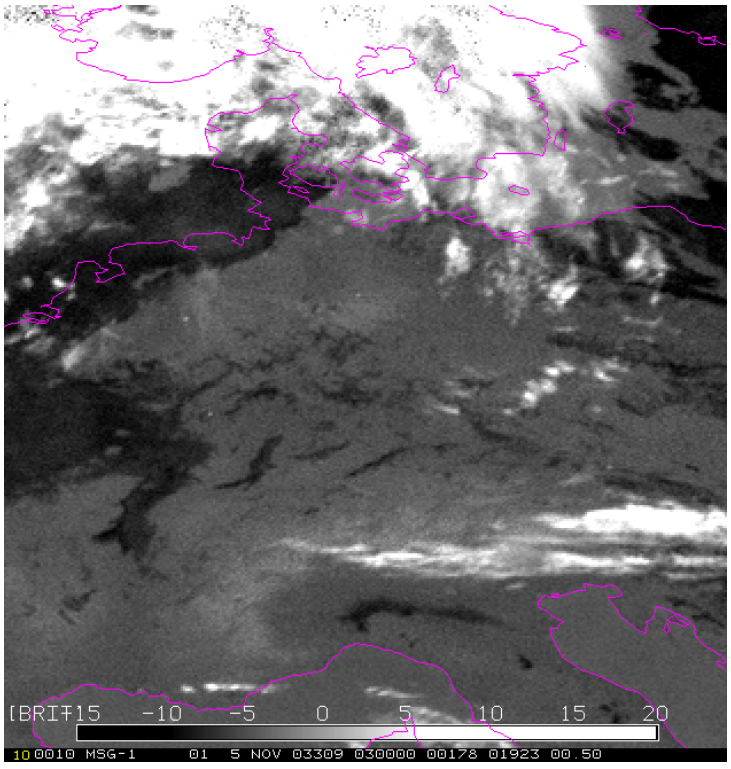

Figure 5: Same as Fig. 4, only temperature difference of IR3.9 – IR10.8 well shows the fog patches in black. (05 November 2003, 0300 UTC)

2.4 Dust and Ash Detection

Detection of desert dust storms and volcanic ash clouds is of utmost importance for flight operations and aviation security, and visibility estimation and health impact monitoring. Again, MSG's multi-spectral capabilities enable a reliable detection of dust and volcanic ash, where the spectral variation of emissivity for dust and ash are exploited. The most important channels in this respect are the so-called split-window channels at IR10.8 and IR12.0, together with the IR8.7 channel. Fig. 6 shows an example of the Dust and Volcanic Ash RGB.

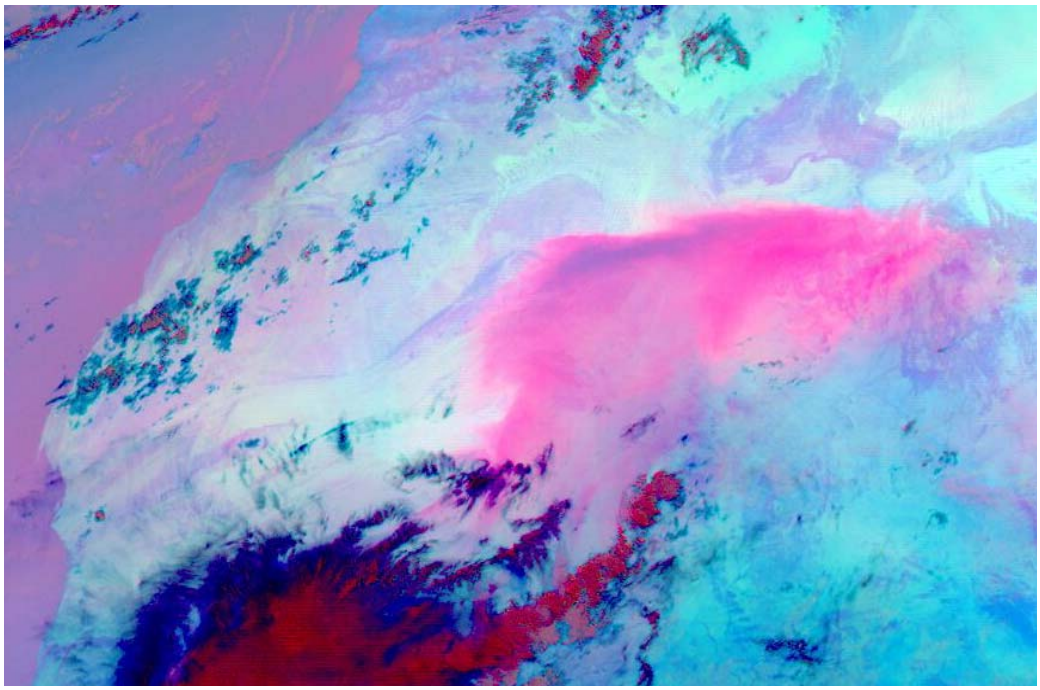

Figure 6: Dust RGB Composite (with the temperature difference IR12.02 – IR10.8 on red, the temperature difference of IR10.8 and IR8.7 on green, and IR10.8 on blue) (03 March 2004, 1000 UTC, MSG image over the Western Sahara). The Saharan dust is well depicted by the magenta colour.

In addition, an objective dust storm and volcanic ash cloud detection algorithm is currently under development at EUMETSAT.

The dust RGB is available on the EUMETSAT website www.eumetsat.int in full resolution over the entire MSG field-of-view.

2.5 The Global Atmospheric Instability Index Product

A new development for the MSG SEVIRI is the derivation of atmospheric instability indices, for the entire MSG field-of-view, which are produced centrally at EUMETSAT's MPEF. The product is known as the Global Instability Index or GII product. The derivation method is based on an optimal estimation technique with the aim to obtain a full temperature and humidity profile from the measurements of 6 SEVIRI infrared channels (WV6.2, WV7.3, IR8.7, IR10.8, IR12.0, IR13.4) together with numerical forecast model profiles as background information. In short, the method tries to change the forecasted profiles in order to obtain a best fit to the MSG measurements in these 6 channels, which means that the final profiles will better reflect the actual and local atmospheric conditions. The profiles are used to infer traditionally well-known, empirical instability indices like the Lifted Index, the K Index, the KO Index and the Maximum Buoyancy.

- Lifted Index $LI = T^{obs} - T^{\text{lifted from surface}}$ at 500 hPa
- K-index $KI = (T^{obs(850)} - T^{obs(500)}) + TD^{obs(850)} - (T^{obs(700)} - TD^{obs(700)})$
- KO index $KO = 0.5 * (\Theta_e^{obs(500)} + \Theta_e^{obs(700)} - \Theta_e^{obs(850)} - \Theta_e^{obs(1000)})$
- Maxim. Buoyancy $MB = \Theta_e^{\text{obs(maximum between surface and 850)}} - \Theta_e^{\text{obs(minimum between 700 and 300)}}$

where T^{obs} is the observed temperature, TD^{obs} is the observed dew point temperature, and Θ_e^{obs} is the observed equivalent potential temperature, all at the indicated pressure level (in hPa).

Furthermore, the total precipitable water content is derived as a fifth parameter for air mass analysis.

A full description of the product and the underlying algorithm can be found in König (2002).

It should be noted, that the profile retrieval is obtained only under cloud free conditions, i.e. the GII product describes the atmospheric instability and thus the potential for convection under still cloud free conditions.

The GII product is derived in a scale of 15 by 15 MSG pixels on a global scale, which corresponds to about 50 by 50 km at the sub-satellite point. Fig. 7 shows an example of the product in this resolution over Europe. Additionally, in support of the international COPS (Convective Orographically-induced Precipitation Study, Wulfmeyer et al. (2007)) experiment, EUMETSAT has started the derivation of a regional instability index (RII) product on a pixel scale over central Europe (Fig. 8).

A global instability product on a higher resolution than the current 15 by 15 MSG pixels is anticipated for the future

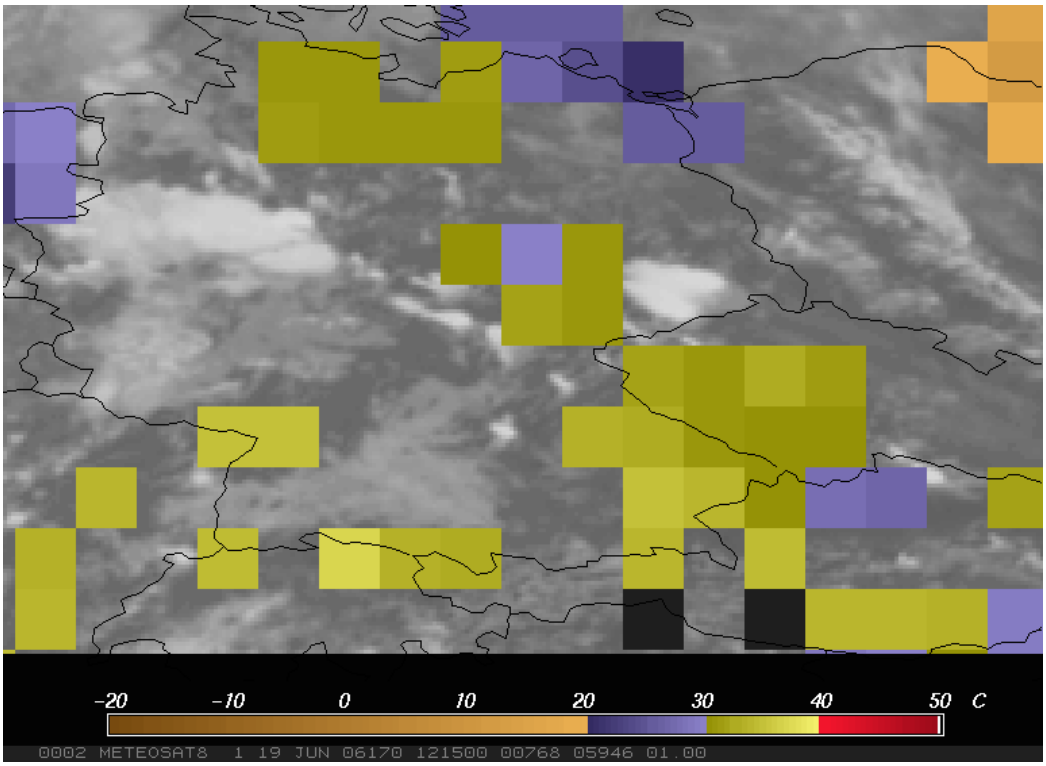

Figure 7: K-Index over Central Europe in the 15 by 15 MSG pixel resolution, as it is done operationally for the full MSG field-of-view (19 June 2006, 1200 UTC)

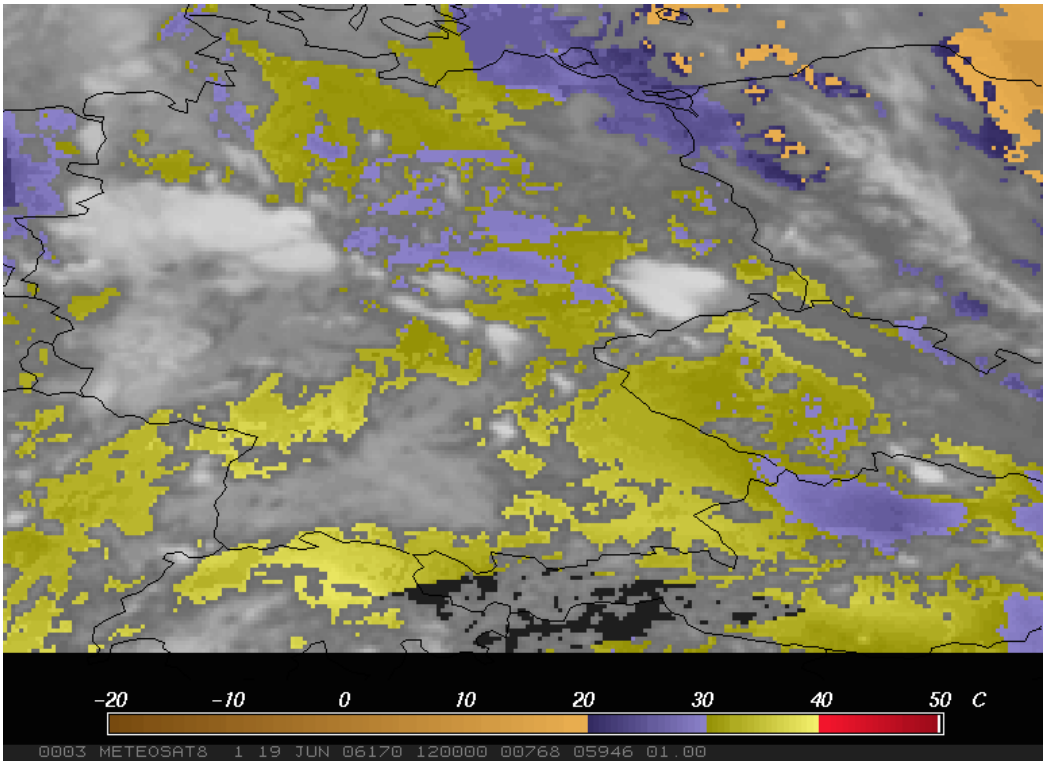

Figure 8: As Fig. 7, but in 1 pixel resolution, as the product is derived as a Regional Instability Index (RII) product over Europe in support of the COPS experiment.

Although numerical models usually well capture the large-scale air mass distribution and thus the general locations of unstable air mass, the additional use of the satellite data can detect the exact strength and local gradients of instability, thus allowing for a more precise forecast of the actual severe weather event. Fig. 9 shows an example of a forecasted K Index in comparison with the satellite derived product, where a stronger instability was found at a position where a severe storm occurred several hours later (de Coning and König, 2006).

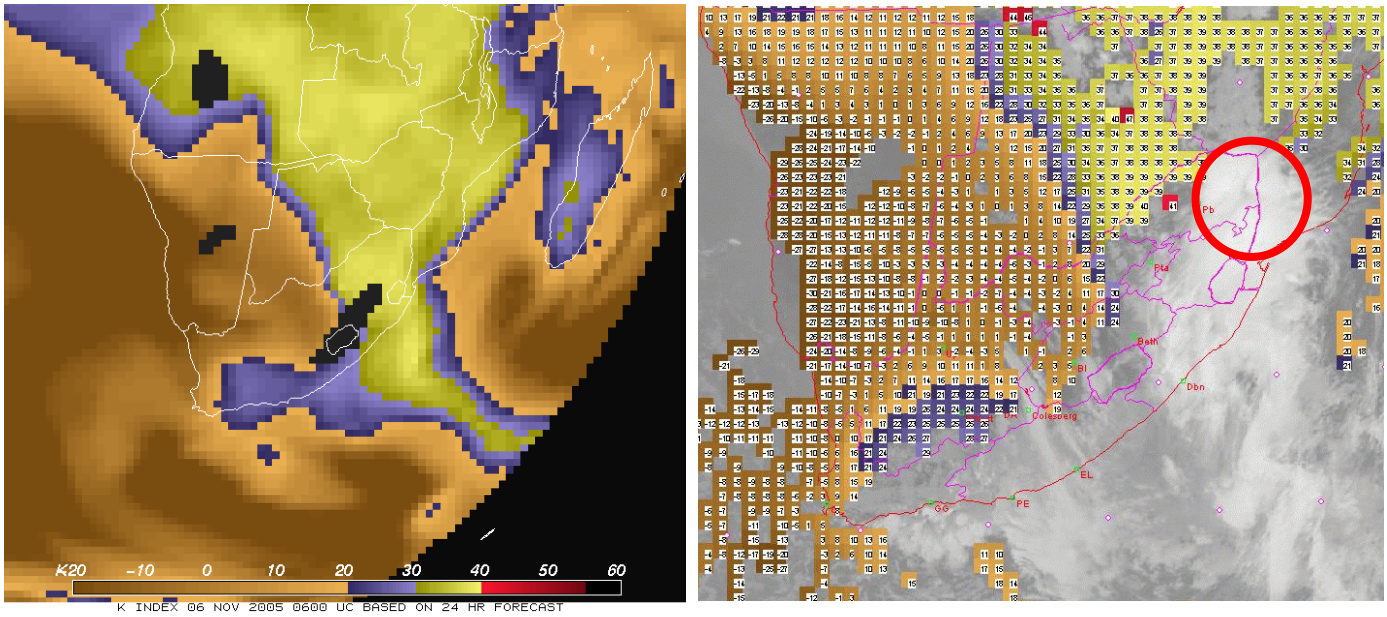

Figure 9: K-Index as derived from the 12-hour ECMWF forecast (left) and from the MSG GII product (right) for the same time (06 November 2005, 0600 UTC): Stronger than forecasted instability is shown by the MSG product in the north-western part of South Africa (indicated by circle). This area experienced a severe storm and tornado at 1430 UTC on the same day.

Many case studies have shown that strong instability is often a precursor of severe convection. The GII product can thus help to identify the convection potential about 6 to 12 hours in advance. (König, 2003). In this context it is very important to mention that the GII product is derived every 15 minutes, so that a continuous monitoring during critical weather situations is ensured.

As an example, the South African Weather Service has carefully evaluated the GII product during the storm season 2006/2007 and has found the success and false alarm rates listed in Table. 2. (de Coning, 2007, personal communication).

Date	Probability of Detection	False Alarm Rate
28 December 2006	0.83	0.21
15 January 2007	0.47	0.31
16 January 2007	0.91	0.42
17 January 2007	0.73	0.33
04 March 2007	0.93	0.38
Average	**0.77**	**0.33**

Table 2.: Example of GII POD and FAR statistics for a few days over South Africa

2.6 Convective Initiation

Once clouds have formed, the MSG SEVIRI measurements allow the assessment whether initially small scale cumuli may grow into severe storms (Bedka and Mecicalski, 2005, and Mecikalski and Bedka, 2006). A semi-operational test version of this product, known as Convective Initiation or CI, has been run over the COPS domain between April and September 2007 (products are available from http://cimss.ssec.wisc.edu/snaap/cops/quicklooks.php.

In short, the CI product first identifies cumulus type of clouds by a textural analysis of the satellite image (Fig. 10). Here the 1 km resolution of the MSG High Resolution VIS channel is the main input information. Once individual cumulus clouds are identified, they are tracked from image to image by a traditional geostationary satellite cloud tracking algorithm, applied to the meso-scale range (Fig. 11)

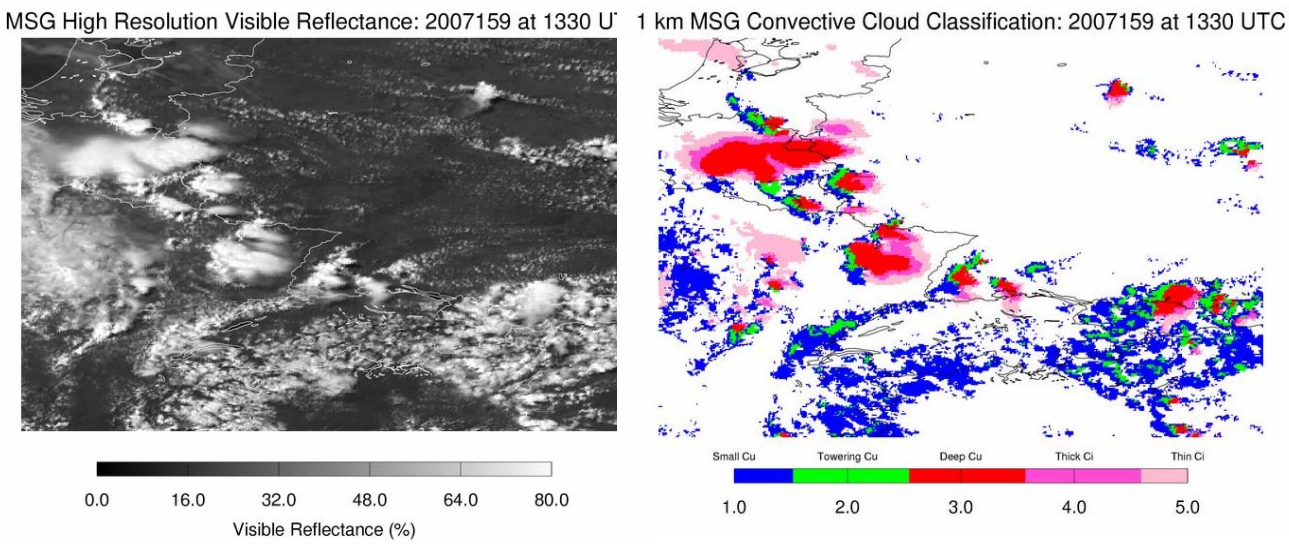

Figure 10: Cloud classification (right) and MSG HRV image (left) for comparison, over the COPS region (SW Germany / Eastern France, Alps)

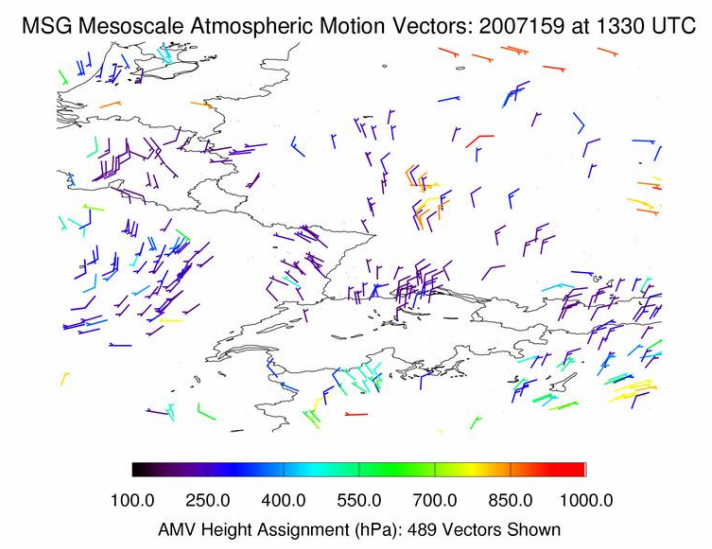

Figure 11: Meso-scale wind field obtained from the MSG data over the COPS region

The such identified cloud elements are then subject to a number of test criteria, all based on SEVIRI measurements in the thermal infrared. Each criterion which is fulfilled by the cloud, adds a certain score to a final severity index or convective initiation index. Table 3 lists these tests for the MSG application:

CI Interest Field	**Critical Value**
IR10.8 temperature TB	< 0 K
IR10.8 TB time trend	< -4K / 15 min and ΔTB / 30 min > ΔTB / 15 min
Timing of IR10.8 TB drop below 0° C	Within prior 30 min
IR8.7 – IR10.8 temperature difference	< 0 K
IR12.0 – IR10.8 temperature difference	- 3 K to 0 K
CAPE (from forecast)	> 500 J/kg

Table 3: CI test criteria for the MSG application (preliminary) (Bedka, 2007, personal communication)

After a certain period, the clouds with highest hit rates in the CI interest fields are identified and e.g. marked red in Fig. 12. The method has been applied to GOES satellite data over the US (with slightly different CI criteria due to the different GOES imager channels) and to MSG data over Europe, and case studies demonstrated that the CI method can detect severe convective clouds up to 45 minutes earlier than weather radar (Fig. 13).

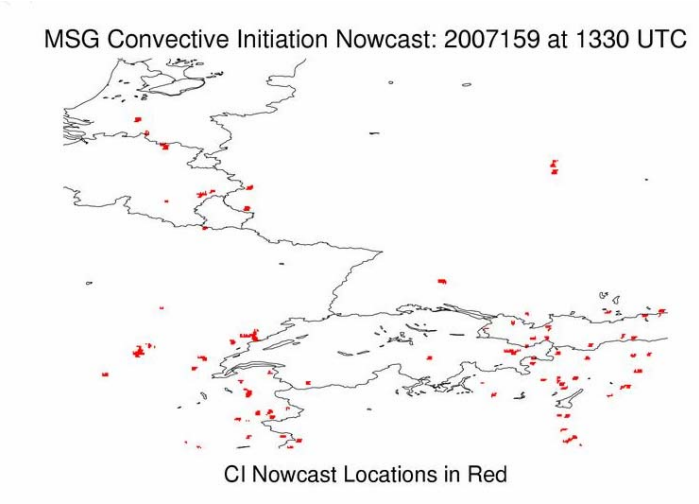

Figure 12: CI locations as a final result of the CI algorithm

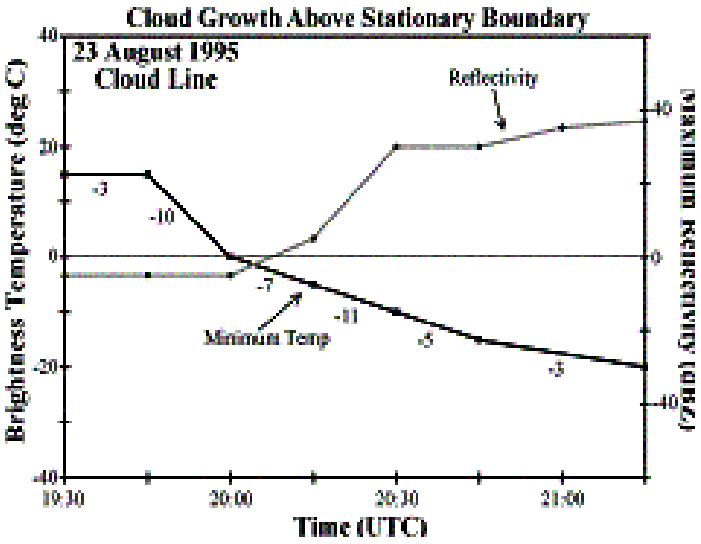

Figure 13: Cloud growth as observed in the IR window channel temperature minimum compared to radar reflectivity gives a warning lead time of ~30 to 45 minutes (Bedka, 2007, personal communication)

As the CI method requires the knowledge of temporal changes (see Table 3), a fast repeat cycle like the 15 minutes SEVIRI data is of crucial importance. Also, the multi-spectral information of SEVIRI allows a refined cloud growth algorithm.

It is the intention to further improve the CI product, especially to capture very rapidly developing storms. Here the even shorter repeat cycle of 5 minutes of the MSG satellite in the so-called rapid scan mode will provide a very useful test data. The MSG rapid scanning was tested in summer 2007 during the COPS field campaign and will probably be operationally available from spring 2008 onwards (for the northern part of the MSG field-of-view). Also, a combination of GII and CI could even enhance the nowcasting value.

2.7 Cloud Microphysics

Some MSG channels are able to detect features resulting from cloud microphysical properties, like cloud optical depth, cloud phase, and particle size as e.g. the effective radius. The relevant channels for cloud microphysics are VIS0.6 (optical depth), NIR1.6 (cloud phase and particle size), the solar component of IR3.9 (particle size), and IR8.7 (cloud phase). The combination of several IR channels can provide precise information on cloud top height.

Already simple channel difference images and RGB composites show these effects: The so-called "True Colour" RGB gives a quick overview of the location of ice clouds (Fig. 14), and the "Convection RGB" (Fig. 15) shows the strong convective cloud tops in bright orange to yellow.

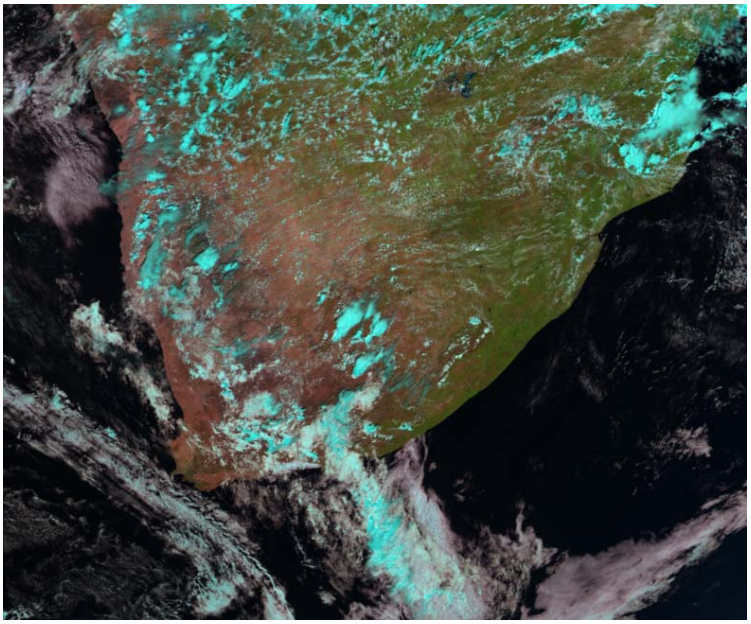

Figure 14: “True Colour” RGB of an MSG image over the Southern part of Africa (with the reflectance of NIR1.6 on red, the reflectance of VIS0.8 on green, and the reflectance of VIS0.6 on blue) (17 January 2007, 1200 UTC). The very low reflectivity of ice in NIR1.6 displays ice clouds in the cyan colour in this composite.

A quantitative exploitation of this image data information has been suggested by Rosenfeld and Lensky (e.g. Rosenfeld and Lensky, 1998). The results of radiative transfer calculations of a number of cloud microphysical parameters and parameter combinations are provided in look-up tables and thus serve as a database for the MSG measurement interpretations in the relevant channels and the respective sun-satellite geometry of the observation point. Using MSG data, Rosenfeld and Lerner (2003) demonstrated the unique capability of these microphysical results to assess the "severeness" of a convective cloud field. Scatter plots of cloud top temperature – as a proxy for cloud top height – and the effective particle size show characteristic patterns, depending on air mass, local aerosol load, and strengths of updrafts (Fig. 16).

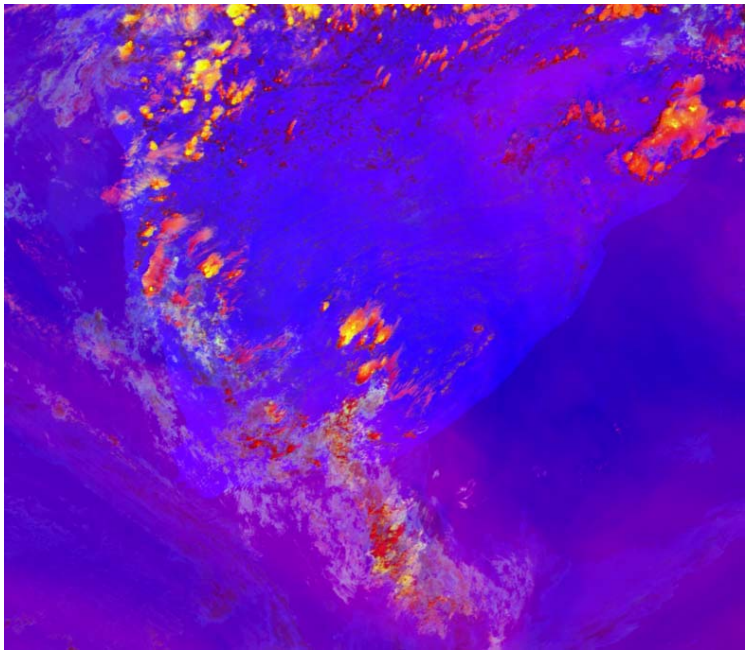

Figure 15: "Convection" RGB over the same region as Fig. 14 (with the temperature difference of WV6.2 – WV7.3 on red, the temperature difference of IR3.9 – IR10.8 on green, and the reflectivity difference of NIR1.6 – VIS0.6 on blue).

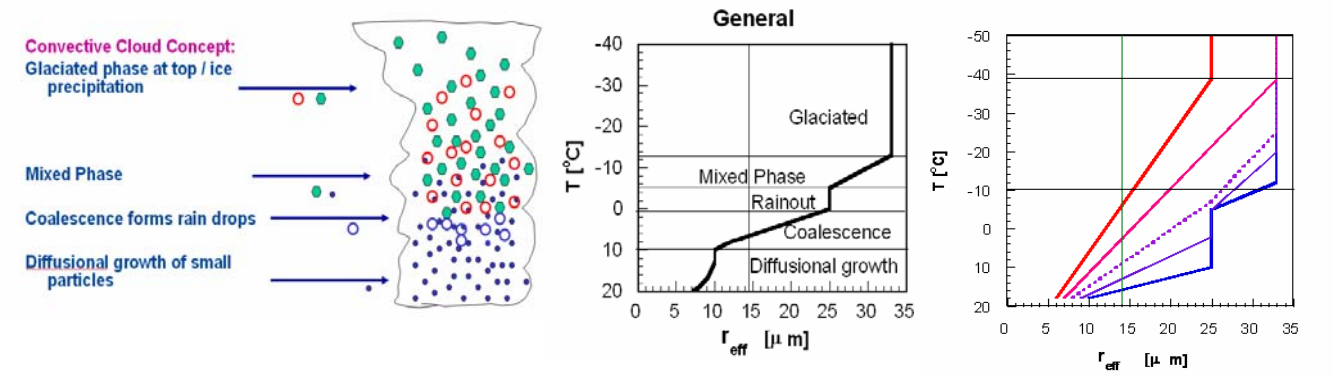

Figure 16: Schematic illustration of the cloud microphysical concept (Rosenfeld, 2003): The different particle sizes and cloud phases within a cloud (left) are translated into a temperature T particle size r_{eff} relationship (centre). Different relations between T and r_{eff} (right) reflect the strengths of updrafts and are thus a measure of how severe the convection is.

Legend for figure on the right: Blue – maritime cloud with weak updraft
Purple - maritime cloud with moderate updraft
Purple, dotted – maritime cloud with strong updraft
Magenta – continental cloud with very strong updraft
Red – continental cloud with extremely strong updraft

A different approach to tackle the derivation of cloud microphysical properties has been developed by EUMETSAT (Watts et al., 1998). The EUMETSAT scheme is based on optimal estimation. Its aim is to find the "optimal" solution for a cloud state vector, where the state variables are cloud top height, cloud phase, effective radius, optical depth, and fractional coverage. "Optimal" solution here means a solution that best fits all MSG measurements in all channels. The specific advantage of this approach is that it corrects for the semi-transparency of clouds and, most important, also provides an error or uncertainty measure for each cloud parameter. The diurnal life cycle of a tropical convective cloud has been successfully calculated by this optimal estimation approach (Fig. 17). The presentation of these results in form of T-r_{eff} plots, as described above, is here of course also possible.

EUMETSAT plans to provide the cloud microphysical data as a centrally derived product in 2008.

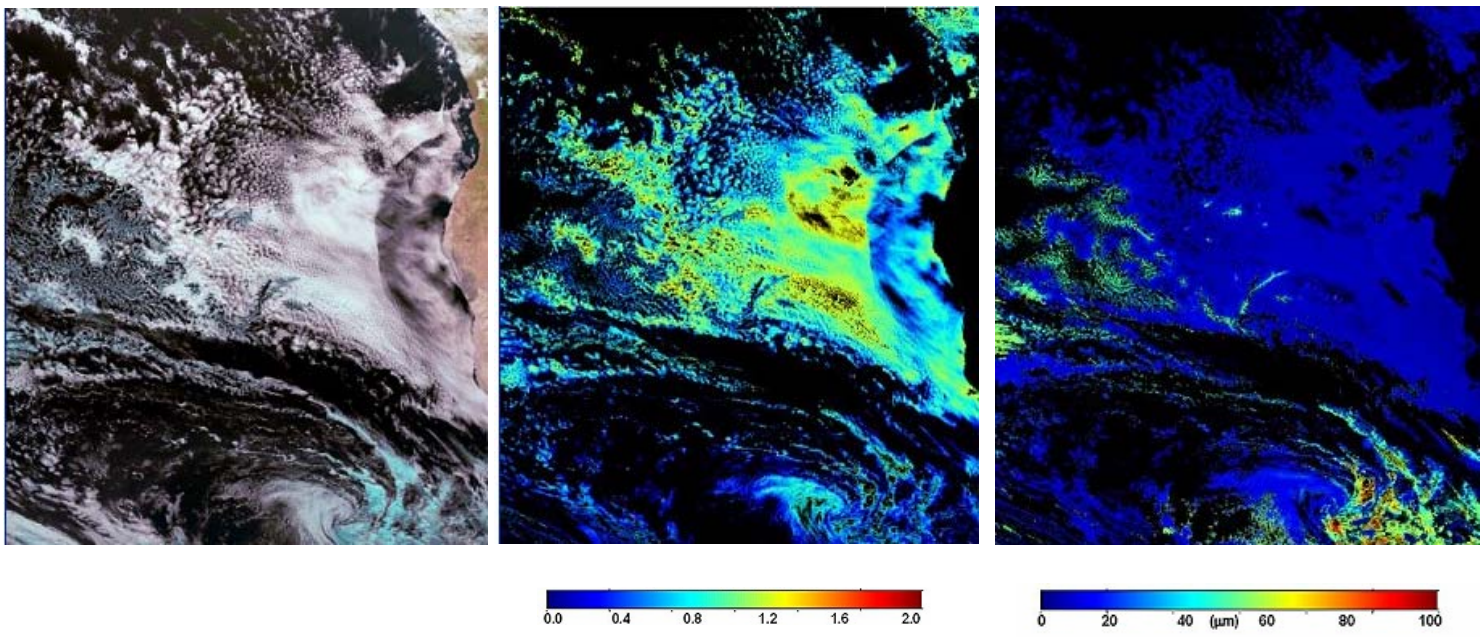

Figure 17: The EUMETSAT cloud microphysical retrieval scheme applied to a marine stratocumulus region over the South Atlantic. Left: “True colour” image for reference, centre: retrieved optical depth, right: retrieved particle size

MSG's 15 minute repeat cycle is an obvious asset for the study of cloud microphysical parameters: The short repeat cycle will in most cases ensure a sufficient analytical tool so that clouds in their most critical convective state can be monitored. Shorter repeat cycles (MSG in rapid scan mode) even enhance this capability.

In summary, the cloud microphysical results show again the combined use of suitable RGB composites, which may serve as quicklooks to identify areas of interest, and then use quantitative products asa further enhanced analysis method.

A new development, which EUMETSAT will pursue in 2008 in co-operation with experts from the US (Cooperative Institute of Meteorological Satellite Studies, CIMSS, at the

University of Wisconsin, and with experts from the University of Alabama), aims at the combination of the cloud microphysical results with the Convective Initiation product

2.8 Estimation of Precipitation

The visible and infrared channels onboard MSG do not allow per se a direct detection of precipitation. Nevertheless, the observations of cloud top properties can be indicative of precipitation. Such indirect methods have been developed and are applied to a number of geostationary satellites (Levizzani et al., 2007). One of EUMETSAT's operational products is the Multisensor Precipitation Estimate (MPE) (Turk et al. 1999, and Heinemann et al. 2002), which uses a combination of geostationary infrared and polar orbiter microwave data. An enhanced version of MPE is the so-called CMORPH blending technique (Joyce et al., 2004). Another method, which just uses the satellite infrared images together with numerical model output, is the Hydroestimator (Scofied and Kuligowski, 2003). EUMETSAT currently investigates the operational use of CMORPH and the Hydroestimator. A more detailed description of the EUMETSAT activities towards quantitative estimation of precipitation is given in CGMS-35-WP-20.

3 CONCLUSIONS

The above description of the products show the wide range of the MSG nowcasting capabilities, from possibilities tovalidate and control the accuracy of numerical weather prediction models with respect to the large scale circulation, e.g. the exact position of cyclones, to pre-convective identification of potentially unstable airmasses and to a detailed analysis of the cloud formation and dissipation processes. Not explicitly mentioned in this paper, but nevertheless also important for some aspects of nowcasting, is the identification of other environmentally important features, as e.g. the detection of floods, wildfires and fire smoke plumes.

MSG’s spectral channels are currently a unique asset for such observations and the derivation of nowcasting products. Together with the 15 minute or at time eves 5 minute repeat cycle the satellite ensures a continuous monitoring of the critical atmospheric processes.

New developments and further enhancement of modern nowcasting products, as e.g. the Convective Initiation product, are possible with MSG. This is also relevant as most of the MSG channels will be available with future geostationary imagers, so that MSG is also a valuable asset in the preparation of future geostationary missions like GOES-R or Meteosat Third Generation.

In conclusion, CGMS is invited to take note and to recommend the enhanced cooperation of CGMS partners in the development of further nowcasting products and techniques, especially considering the advanced utilisation of current and future geostationary satellite systems (METEOSAT, GOES, MTG, GOES-R etc.).

References

Bedka, K. M., and J. R. Mecikalski, 2005: Application of satellite-derived atmospheric motion vectors for estimating mesoscale flows. *J. Appl. Meteor.* , **44**, 1761-1772

de Coning, E. and M. König, 2006: MSG for nowcasting – experiences over Southern Africa. *Proc. of the 2006 EUMETSAT Meteor. Sat. Conf.*

Heinemann, T., A. Lattanzio, and F. Roveda, 2002: The EUMETSAT multi-sensor precipitation estimate (MPE). *Proc. Sec. Int'l. Prec. Working Group (IPWG)*

König, M., 2002: Atmospheric instability parameters derived from MSG SEVIRI observations. EUM TM 09, EUMETSAT, available from http://www.eumetsat.int/groups/ops/documents/document/pdf_tm09_msg_instab-params.pdf.

König, M., 2003: Atmospheric instability parameters derived from MSG SEVIRI observations. *Proc. of the 2003 EUMETSAT Meteor. Sat. Conf.*, 155-161

König, M., 2007: The global instability indices product: Algorithm theoretical basis document. EUM.MET.REP.07, EUMETSAT, available from http://www.eumetsat.int/groups/ops/documents/document/pdf_met_atbd_gii.pdf.

Levizzani, V., P. Bauer, and F.J. Turk, 2007: Measuring precipitation from space: EURAINSAT and the future. Springer Netherlands, 722 pp.

Mecikalski, J. R., and K. M. Bedka, 2006: Forecasting convective initiation by monitoring the evolution of moving convection in daytime GOES imagery. *Mon. Wea. Rev*. **134**, 49-78

Rosenfeld, D. and I. Lensky (1998): Satellite-based insights into precipitation formation processes in continental and maritime convective clouds. *Bull. Amer. Met. Soc*., **79**, 2457-2476

Rosenfeld, D. and A. Lerner (2003): Satellite multi-spectral identification of severe storms and their nowcasting by the micro-structure of the pre-storm clouds. *Proc. of the 2003 EUMETSAT Meteor. Sat. Conf.*, 334

Schmetz, J., P. Pili, S. Tjemkes, D. Just, J. Kerkmann, S. Rota, and A. Ratier, 2002: An introduction to Meteosat Second Generation (MSG). *Bull. Amer. Met. Soc*., **83**, 977 – 992

Scofied, R.A. and R.J Kuligowski, 2003: Status and outlook of operational satellite precipitation algorithms for extreme precipitation events. *Wea. and Forecasting*, **18**, 1037-1051

Turk, F.J., G.D. Rohaly, J. Hawkins, E.A. Smith, F.S. Marzano, A. Mugnai, and V. Levizzani, 1999: Meteorological applications of precipitation estimation from combined SSM/I, TRMM and infrared geostationary satellite data. *Microwave Radiometry and Remote Sensing of the Earth's Surface and Atmosphere*, P. Pampaloni and S. Paloscia Eds., VSP Int. Sci. Publ., 353-363

Watts, P.D. C.T. Mutlow, A.J. Baran, and A.M. Zavody, 1998: Sutdy on cloud properties derived from Meteosat Second Generation observations. EUM IRR 97-181, http://www.eumetsat.int/groups/ops/documents/document/pdf_sci_97181_msg-cloud-props.pdf

Wulfmeyer, V., et al., 2007: The Convective and orographically-induced precipitation study: A research and development project of the world weather research program for improving quantitative precipitation forecasting in low-mountain regions. To be published in *Bill. Amer. Met. Soc.*